



Contents lists available at ScienceDirect

## Organic Geochemistry

journal homepage: [www.elsevier.com/locate/orggeochem](http://www.elsevier.com/locate/orggeochem)

## Insights into preservation of fossil plant cuticles using thermally assisted hydrolysis methylation

Anne-Marie Aucour<sup>a,\*</sup>, Pierre Faure<sup>b</sup>, Bernard Gomez<sup>c</sup>, Yann Hautevelle<sup>d</sup>, Raymond Michels<sup>b</sup>, Frédéric Thévenard<sup>c</sup>

<sup>a</sup> Laboratoire des Sciences de la Terre, CNRS-UMR 5570, Ecole Normale Supérieure de Lyon, Université Lyon 1, 2 rue Dubois, 69622 Villeurbanne Cedex, France

<sup>b</sup> Géologie et Gestion des Ressources Minérales et Énergétiques (G2R), UMR 7566, Nancy Université, CNRS BP 239, 54506 Vandoeuvre-les-Nancy Cedex, France

<sup>c</sup> Paléoenvironnements Paléobiosphère (PEPS), CNRS-UMR 5125, Université Lyon 1, 7 rue Dubois, 69622 Villeurbanne Cedex, France

<sup>d</sup> Géologie et Gestion des Ressources Minérales et Énergétiques (G2R), UMR 7566, Nancy Université, CNRS BP 40, 54506 Vandoeuvre-les-Nancy Cedex, France

### ARTICLE INFO

#### Article history:

Received 2 January 2008

Received in revised form 3 March 2009

Accepted 17 April 2009

Available online 24 April 2009

### ABSTRACT

The chemical composition of Cretaceous leaf remains showing exceptionally well preserved cuticles was investigated using pyrolysis gas chromatography–mass spectrometry (Py-GC–MS) and thermally assisted hydrolysis methylation (THM)–GC–MS. Samples of Coniferales (*Frenelopsis*) and Ginkgoales (*Nehvizdya penalveri*) leaf remains were collected from freshwater and coastal marine depositional environments. Material for pyrolysis included (i) untreated leaves and cuticles obtained after extraction from mineral rock matrix and bleaching, (ii) kerogen fraction from both materials, (iii) non-hydrolysable fraction from kerogen. The THM–GC–MS data from untreated leaves and bleached cuticles show that the fossil cuticle geopolymer essentially released aliphatic components upon thermal treatment, with a dominance of fatty acids (FAs) and *n*-alkanes/*n*-alkenes. The FAs are essentially resistant to bleaching and remain after solvent extraction. They occur mainly as short chain compounds ranging from C<sub>6</sub> to C<sub>16</sub> and with maximum abundance at C<sub>8</sub>–C<sub>9</sub>. The *n*-alkanes/*n*-alkenes from kerogen and the non-hydrolysable residue occur mainly as short chain compounds in the range C<sub>10</sub>–C<sub>16</sub>, with the highest abundance at C<sub>9</sub>–C<sub>12</sub>. The THM–GC–MS pyrograms of the fossil cuticles differ from those of cutan from fresh living plants. They support the preservation model via polymerization of monomers derived from cutin or from unsaturated cell FAs.

© 2009 Elsevier Ltd. All rights reserved.

### 1. Introduction

The occurrence of fossil plant cuticles in sedimentary rocks has raised questions about the processes of preservation of the cuticle and about their contribution to the formation of kerogen (Nip et al., 1986; Möhle et al., 1998). Selective preservation of the biopolymer cutan was invoked to explain the predominance of long chain *n*-alkanes/*n*-alkenes in fossil cuticles upon conventional Py-GC–MS (Nip et al., 1986; Tegelaar et al., 1991; Briggs, 1999). The widespread occurrence of cutan in plant cuticle is, however, a matter of debate (Möhsle et al., 1997; Boom et al., 2005; Gupta et al., 2006). In situ polymerization has alternatively been proposed to account for the chemical transformation and preservation of the cuticle with diagenesis (de Leeuw et al., 2006). It has been thought to involve the formation of ether bonds via intermolecular reaction of alcohol and epoxy groups in the cutin monomers (Tegelaar et al., 1991), the bonding of aromatic moieties to otherwise labile aliphatic cuticular components (Kögel-Knabner et al., 1994; Möhsle

et al., 1998) and/or the polymerization of aliphatic moieties derived from cutin and wax components (Möhsle et al., 1998; Finch and Freeman, 2001; Gupta et al., 2007a–c).

Investigation of the chemical structure of fossil cuticles appears crucial for such topics (Tegelaar et al., 1991; Möhsle et al., 1998; Stankiewicz et al., 2000; Gupta et al., 2007a,b). This has essentially relied on conventional flash pyrolysis Py-GC–MS in combination with solid state <sup>13</sup>C nuclear magnetic resonance (NMR) spectroscopy or infrared spectroscopy (Nip et al., 1986; Tegelaar et al., 1991; Möhsle et al., 1998; Almendros et al., 1999; Gupta et al., 2008). Conventional Py-GC–MS has been carried on fossil leaf and cuticle that were either untreated (Nip et al., 1986; Tegelaar et al., 1991; Almendros et al., 1999) or separated from the mineral rock matrix using HF, HCl and extracted with solvent (Möhsle et al., 1997, 1998; Almendros et al., 1998). The effects of these treatments on the products released upon pyrolysis have not been tested yet. Furthermore, non-cuticular coalified residues derived from shoot lignin may release aromatic moieties seen in the pyrograms (Almendros et al., 1998; Möhsle et al., 1998). They are removed, for instance, by oxidative maceration (Kerp, 1990) before observation under light, scanning electron and transmission electron microscopy. The effect of oxidative maceration on the

\* Corresponding author. Tel.: +33 4 72 44 84 16; fax: +33 4 72 44 85 93.  
E-mail address: [aucour@univ-lyon1.fr](mailto:aucour@univ-lyon1.fr) (A.-M. Aucour).

macromolecular composition of fossil cuticle has, however, not been investigated.

Flash Py-GC-MS with in situ methylation using tetramethylammonium hydroxide (TMAH) has rarely been applied to fossil plants (Almendros et al., 1998; Gupta et al., 2007b,c). The thermally assisted hydrolysis methylation (THM; Challinor, 1994) induced by TMAH is particularly effective in transforming insoluble macromolecular material composed of esters and phenolic polymers to monomers by way of hydrolysis and subsequent alkylation (Challinor, 1989, 1991). It appears to be a particularly suitable technique for investigating the structure of cuticular biopolyesters and esters (de Leeuw and Baas, 1993; McKinney et al., 1996; del Rio and Hatcher, 1998) and their preservation state in fossil plants, complementing existing analysis (Almendros et al., 1998; Gupta et al., 2007b,c).

Cuticle remains of the Cretaceous Coniferales and Ginkgoales provide a material of choice for investigating the chemical structure of fossil cuticle and its preservation. The Cheirolepidiaceae conifers were important components of Mesozoic flora and terrestrial biomass. They extended in a broad zone between 40°N and 40°S (Skelton, 2003). Their thick cuticles were thought to prevent water loss in dry or saline environments (Watson, 1977). Abundant and well-preserved cuticles of the Cheirolepidiaceae species *Frenelopsis* were collected from freshwater fluvio-lacustrine and coastal marsh deposits (Gomez et al., 2001, 2002). They are associated with those of *Nehvizdya* (Ginkgoales) in a brackish coastal environment. The main objectives were to document (i) the chemical structure and preservation of cuticles of Coniferales (*Frenelopsis*) and Ginkgoales (*Nehvizdya*) embedded in the same rock layer and (ii) the influence of pre-treatment used prior to pyrolysis to remove cuticle from mineral rock matrix to bleach it, in order to isolate the kerogen fraction. The structure of fossil cuticle was investigated using flash Py-GC-MS with and without TMAH as THM induced by TMAH was found very effective in transforming insoluble macromolecular material composed of esters and phenolic polymers, in particular cutin. In addition, kerogen from fossil leaf and cuticle was subject to base hydrolysis prior to pyrolysis in order to investigate the non-hydrolysable macromolecular component.

## 2. Materials and methods

The material includes *Frenelopsis* remains from freshwater intra-continental and brackish coastal environments; in the latter case, *Frenelopsis* is associated with *Nehvizdya*. The lithology and depositional environments of the rock samples and the preparation of the cuticles are presented in Fig. 1. One sample (Uña-3) was collected from a section of the La Huérguina Formation (Uña, Southwestern Iberian ranges, Spain) dated from the Upper Barremian and which records a cycle of deltaic progradation-retrogradation on the margin of a lake (Gomez et al., 2001). The second sample (Rubielos) was collected from the lower member of the Escucha Formation (Rubielos de Mora, Eastern Iberian ranges, Spain) dated from Lower to Middle Albian and which corresponds to sedimentation in a deltaic front and in brackish marshes bordering the tidal flats of the lower deltaic plain of the huge Escucha delta (Gomez et al., 2002).

Cuticular remains were obtained in two ways. In the first, leaf remains were directly scraped from the rock matrix with a razor blade (referred to herein as untreated leaf or untreated material or untreated cuticle). The dark-coloured leaf remains obtained in this way actually consist of cuticles plus their internal non-cuticular residues. In the second, plant cuticle was extracted from the rock and bleached using common procedures (Kerp, 1990). The procedure for cuticle extraction from rock depends on the type of rock matrix and involved maceration with 0.5–1 N HCl in the case of carbonate lignite (Uña-3) or with H<sub>2</sub>O<sub>2</sub> (18–37%) in the case of

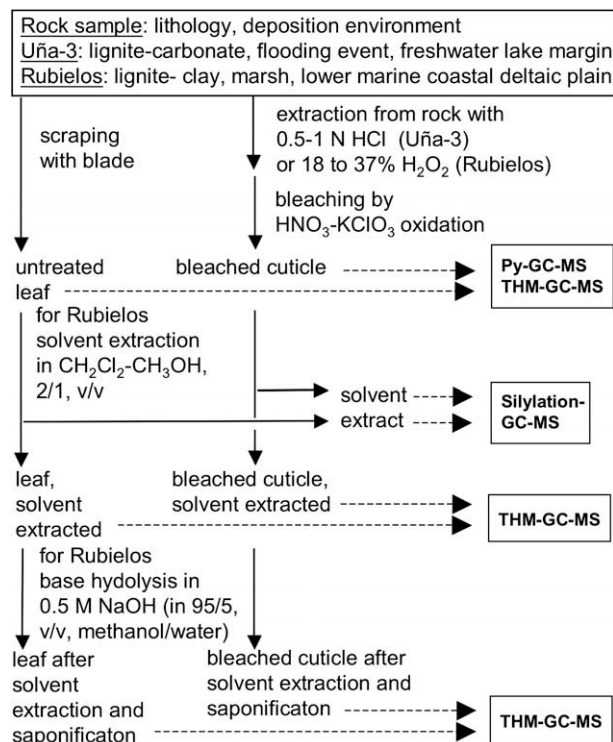


Fig. 1. Depositional environment, enclosing lithology and preparation method for material studied.

clayey lignite (Rubielos). The dark-coloured cuticular remains left after maceration were bleached in a saturated solution of KClO<sub>3</sub> in HNO<sub>3</sub> (60%; Kerp, 1990) and washed with deionised water. The cuticles obtained are referred to herein as bleached cuticles. Extraction from rock and bleaching makes cuticular material suitable for morphological observation under light, scanning (and transmission) electron microscopy.

Samples of untreated leaves (ca. 30 mg) and bleached cuticles (ca. 8 mg) of *Frenelopsis turoleensis* from Rubielos were crushed and subjected to solvent extraction and saponification. Solvent-extracted material was obtained after six successive extractions with CH<sub>2</sub>Cl<sub>2</sub>/CH<sub>3</sub>OH (2/1, v/v). Each extraction was performed at ambient temperature for 30 min. The resulting extract was evaporated under N<sub>2</sub> and weighed. Base hydrolysis was performed on the solid residue left after solvent extraction in 0.5 M NaOH (in 95/5 v/v MeOH, MeOH/water) for 2 h at 70 °C (Gupta et al., 2007b).

Samples for flash Py-GC-MS were loaded into quartz tubes and heated at 620 °C for 20 s under an inert atmosphere using a CDS 2000 pyroprobe as described by Faure et al. (2006). The products were analyzed on line using GC-MS (HP 5890 Series II gas chromatograph coupled to a HP 5971 mass spectrometer) with a split-splitless injector, a J&W DB-5 fused silica column (60 m × 0.25 mm i.d., 0.1 mm film thickness). After cryofocussing (–30 °C), the GC oven was programmed to 40 °C at 10 °C/min and 40–300 °C (hold 10 min) at 5 °C/min at a constant He flow (1.4 ml/min). Flash pyrolysis with in situ methylation was carried out according to the procedure of Hatcher and Clifford (1994) by adding solid TMAH to the sample (10/1, w/w) prior to pyrolysis. The mixture was placed in a quartz tube and THM-GC-MS was carried out using the same Py-GC-MS apparatus as described above. On line pyrolysis at 620 °C was performed for 20 s. After cryofocussing (0 °C) for 1 min, the oven temperature programme was: 0 °C (1 min), 70 °C/min to 40 °C (hold 6 min), then 6 °C/min to 300 °C (hold 20 min) with a constant He flow (1.4 ml/min). This procedure avoids thermal destruction and sorption of polar

molecules (i.e. FAs) in the GC injector. Derivatization during pyrolysis results in the methylation of active organic functions (e.g. –COOH groups).

Integration of mass chromatograms with relevant  $m/z$  values was performed and the peak areas were multiplied by a correction factor which takes into account differences in MS response for various compounds. The correction factor was calculated from the mass spectrum of each authentic compound by taking the inverse of the percentages of the total ion current of the relevant  $m/z$  value and multiplying by 100 (Hartgers et al., 1992; Ishiwatari et al., 1995). As a result of this mathematical procedure, distribution patterns were obtained showing the relative concentrations of the different compounds. It should be noticed that the semiquantitative values obtained by integration of chromatographic area are only an indication of the relative abundances of the compounds in each pyrogram.

Organic extracts from  $\text{CH}_2\text{Cl}_2$ – $\text{CH}_3\text{OH}$  extraction were analyzed using GC–MS (HP 5980 Series II coupled to a HP 5972 mass spectrometer, with split–splitless injector, a 60 m DB-5 J&W, 0.25 mm i.d., 0.1  $\mu\text{m}$  film fused silica column. The temperature programme was 60–130 °C at 15 °C/min, then 130–310 °C (hold 17 min) at 3 °C/min (constant He flow of 1 ml/min). Because of the presence of alcohols and carboxylic acids, silylation using BSTFA + TMCS (99/1) was carried out to improve GC resolution (Wenclawiak et al., 1993; Kokinos et al., 1998). The dried extract was dissolved with the derivatizing solution and heated (15 min at 60 °C); 1  $\mu\text{l}$  of the solution was directly injected into the gas chromatograph.

### 3. Results

#### 3.1. Morphology and histology

The material consists of morphologically well preserved leafy remains, along with cuticles showing (Fig. 2) clear epidermal and stomatal cell structures (Gomez et al., 2000, 2001, 2002). As

evidence of excellent preservation, whole oblanceolate to lanceolate, translucent leaves of *Nehvizdya penalveri* from Rubielos exhibit clear vein trajectories that are several times dichotomised in the basal lamina part, parallel in the mid-lamina, and convergent in the apical lamina (Fig. 2a and b). Small flattened globular to spindle-shaped resin bodies are located between veins (Fig. 2c). Note that, in the case of *Nehvizdya*, veins and resin bodies were present inside the leaf lamina and remained contained between the cuticles even after bleaching. Both abaxial and adaxial leaf cuticle outer surfaces are smooth and undamaged, except at the level of the stomata, which are surrounded by a slightly elevated ring. Inner surfaces show well preserved cellular patterns with delicate anticlinal walls separating epidermal cells from subsidiary and guard cells.

Branched vegetative shoots of *Frenelopsis* were found several times from the same sedimentary layer, the high degree of morphological connections likely indicating short distance of deposition and calm transport. The axis is made of cuticle cylinders usually containing amorphous, dark organic residues. Each cylinder bears short free tips that show thick external abaxial cuticles (at least 20  $\mu\text{m}$  thick) and thin internal adaxial cuticles (ca. 5  $\mu\text{m}$  thick). This is interpreted as either internode-bearing short leaves by comparison with the living angiosperm *Salicornia* or the basal sheathing part of leaf abaxial surface, by comparison with living scale-leafed conifers (Daviero et al., 2001); it is referred to here as leaf. The outer cuticle surfaces are not only sculptured with the stomata but also by the inner and outer papillae borne by the subsidiary cells and, depending on the species considered, by a range in size and number of papillae and hairs borne by the epidermal cells and more or less extended on the surface (Fig. 2d–f). Inner surfaces show well preserved cellular patterns with delicate anticlinal walls separating epidermal cells from subsidiary and guard cells (Fig. 2d and e). Light and scanning electron microscopy (SEM) observations of the cuticles led us to recognize two different morphospecies of *Frenelopsis*: *Frenelopsis uñaensis* (Uña-3) and *F. turoloensis* (Rubielos).

#### 3.2. Chemical composition

Total ion current (TIC) chromatograms were compared for Py-GC–MS with and without in situ methylation with TMAH. Results are shown for untreated leaves of *N. penalveri* (Figs. 3–5) and *F. turoloensis* (Figs. 5 and 6) from Rubielos and for bleached cuticle of *F. turoloensis* from the same rock layer (Figs. 5 and 7). The TIC from conventional Py-GC–MS of untreated *N. penalveri* leaf from Rubielos shows prominent series of *n*-alkanes/*n*-alkenes and aromatic compounds (Fig. 3a; Table 1). Highest relative abundances of *n*-alkanes/*n*-alkenes (with double bond at  $\omega$ -position) are observed at  $\text{C}_{27}$ – $\text{C}_{29}$  and at  $\text{C}_9$ – $\text{C}_{12}$  for the shorter chain homologues as shown by the  $m/z$  57 chromatogram (Fig. 3b). The long chain homologues from  $\text{C}_{25}$  to  $\text{C}_{32}$  have a marked odd/even predominance. The pyrograms show weak but conspicuous alkan-2-one peaks in the range  $\text{C}_6$ – $\text{C}_{18}$  (max. at  $\text{C}_{10}$ ). Prominent aromatic compounds are benzene and alkyl benzenes, naphthalene and alkyl naphthalenes, phenanthrene and alkyl phenanthrene, phenol and methylphenol. Upon pyrolysis with TMAH (Fig. 4a), series of methyl esters (MEs) of FAs emerge, yet the distributions of the *n*-alkanes/*n*-alkenes remain similar (Fig. 4b). The MEs of alkanic and alkenic acids have a normalized ratio to *n*-alkanes/*n*-alkenes of 1.37 for untreated *Nehvizdya* material. They have prominent peaks from  $\text{C}_5$  to  $\text{C}_{16}$ , maximizing at  $\text{C}_8$ – $\text{C}_9$  and to a lesser extent at  $\text{C}_{16}$ , as shown by the  $m/z$  74 chromatogram (Fig. 4c). Longer chain alkanic MEs show smaller peaks up to  $\text{C}_{28}$ , with marked even/odd predominance and with relative maximum at  $\text{C}_{26}$ . MEs of  $\alpha$ - $\omega$ -alkanedioic acids are present in very low abundance, in the range  $\text{C}_7$ – $\text{C}_{12}$ . Trace amounts of

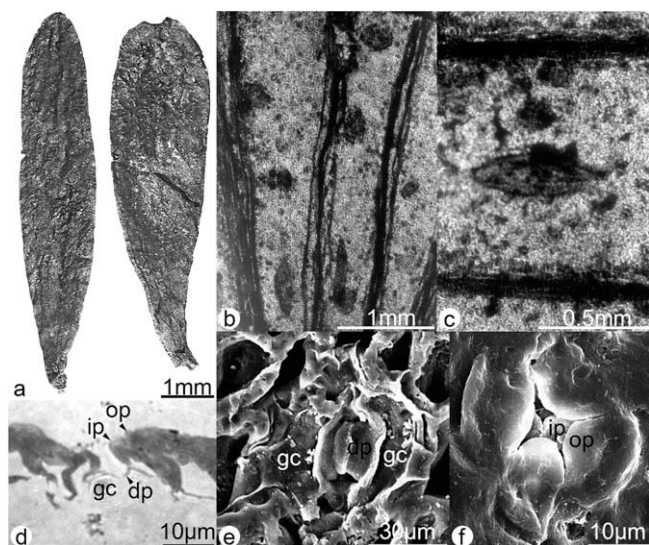


**Fig. 2.** Light microscopy and SEM of plant material from Rubielos and Uña-3. (a) Two entire leaves of *Nehvizdya penalveri* showing petiolarly cunate bases and oblanceolate or obovate blades. Light microscopy observations with details of (b) round, oval and spindle-shaped resin bodies located between the veins in the mesophyll and (c) spindle-shaped resin body positioned parallel to the veins. (d) Thin section of leaf cuticle of *Frenelopsis turoloensis* across a stoma and epidermal cells with inner papillae ip, outer papillae op, guard cells gc, and dorsal plates dp. SEM of (e) internal view of *Frenelopsis uñaensis* stoma with two well preserved dorsal plates dp closing the stomatal pit arising from two guard cells gc and (f) external view of *Frenelopsis turoloensis* stoma showing inner papillae underneath massive outer papillae.

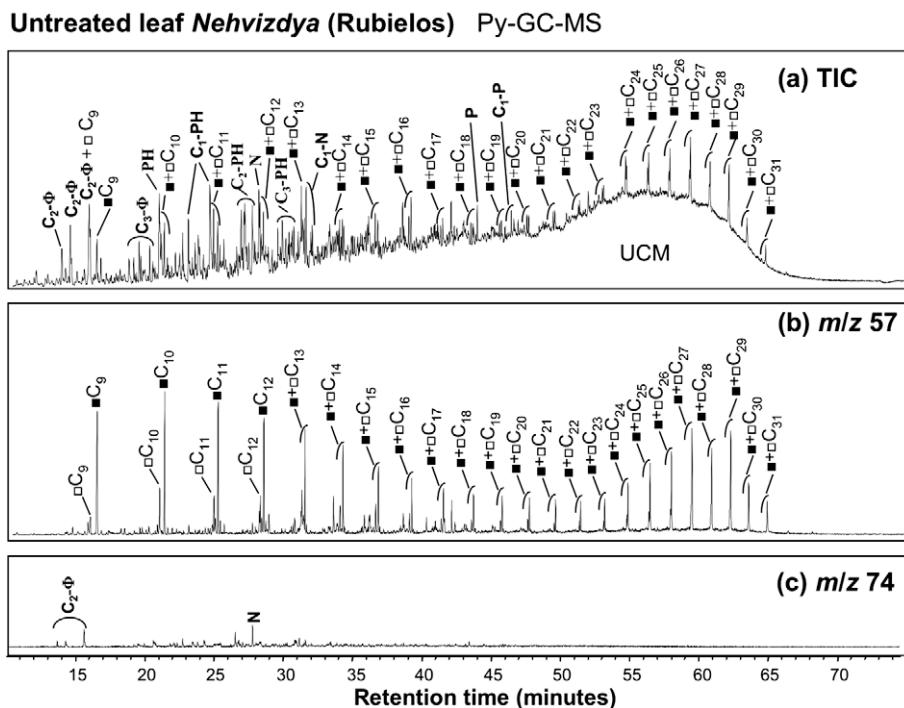


**Fig. 3.** Pyrograms of untreated leaf of *Nehvizdya penalveri* from Rubielos without TMAH: (a) TIC chromatogram, (b)  $m/z$  57 and (c)  $m/z$  74 chromatograms.

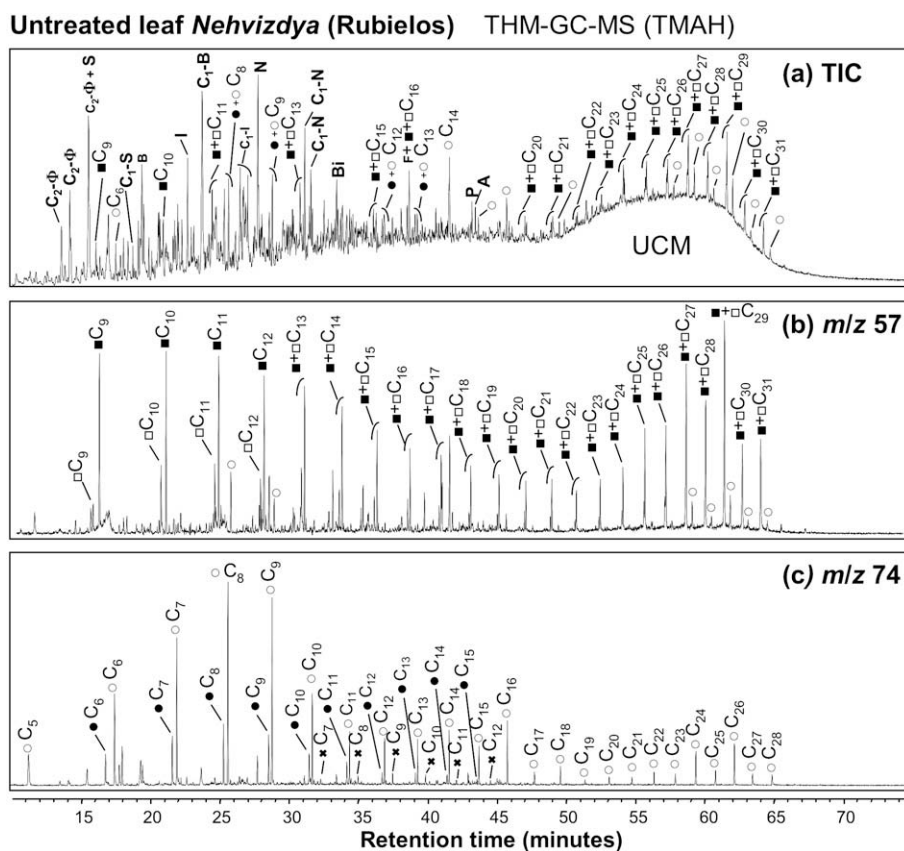


**Fig. 4.** Pyrograms of untreated leaf of *Nehvizdya penalveri* from Rubielos with TMAH: (a) TIC chromatogram, (b)  $m/z$  57 and (c)  $m/z$  74 chromatograms.

alkan-2-ones ranging from  $C_7$  to  $C_{11}$  are also present. In addition to the release of additional FAMES, in situ methylation with TMAH affected the aromatic assemblages (Fig. 5b). Phenol, methylphenol,

naphthalene, methyl naphthalene and phenanthrene dominated the aromatic assemblage from conventional Py-GC-MS, while benzaldehyde and alkyl benzaldehydes were dominantly produced

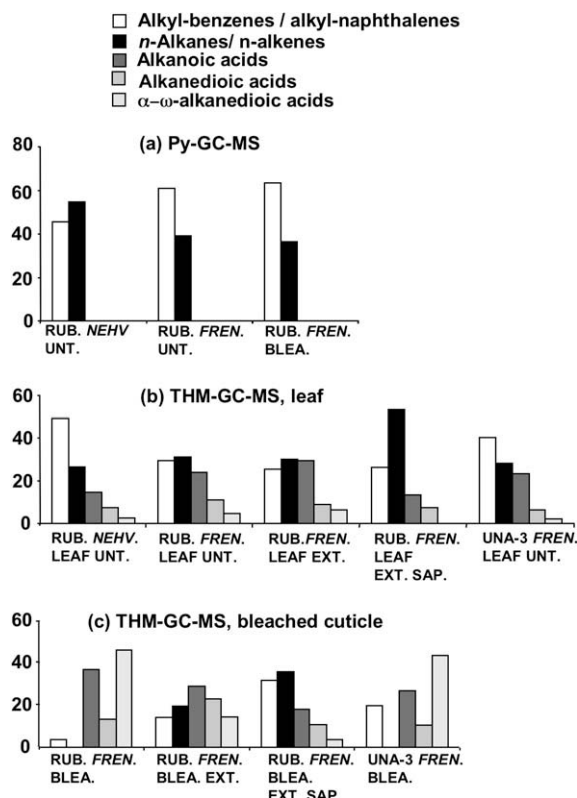


**Fig. 5.** Relative proportions (%) of selected aromatic compounds and selected aliphatic compounds released upon pyrolysis without and with TMAH. Selected aromatic compounds are alkyl benzenes, alkyl naphthalenes. Selected aliphatic compounds are *n*-alkanes/*n*-alkenes upon Py-GC-MS; they additionally include FAMES and  $\alpha$ - $\omega$ -alkanedioic acid MEs upon THM-GC-MS. Abbreviations are NEHV.: *Nehvizdya*, FREN.: *Frenelopsis*, RUB.: Rubielos, UNT.: untreated, BLEA.: bleached, EXT.: solvent extracted, SAP.: after saponification.

**Table 1**  
Components in pyrograms in Figs. 3, 4 and 6–9, and Appendices 1 and 2.

Symbol	Compound
*C <sub>i</sub>	Alkanedioic acid ME <sup>a</sup> ( <i>i</i> = C number)
○C <sub>i</sub>	Alkanoic acid ME <sup>a</sup> ( <i>i</i> = C number)
●C <sub>i</sub>	Alkenoic acid – DME <sup>b</sup> ( <i>i</i> = C number)
C <sub>i</sub> - $\Phi$	Alkyl benzene ( <i>i</i> = C number)
■C <sub>i</sub>	<i>n</i> -Alkane ( <i>i</i> = C number)
□C <sub>i</sub>	<i>n</i> -Alk-1-ene ( <i>i</i> = C number)
S	Styrene
C <sub>i</sub> -S	Alkyl styrene ( <i>i</i> = C number in alkyl chain)
B	Benzaldehyde
C <sub>i</sub> -B	Alkyl benzaldehyde ( <i>i</i> = C number in alkyl chain)
Ba-ME	Benzoic acid ME <sup>a</sup>
N	Naphthalene
I	Indene
C <sub>i</sub> -I	Alkyl indene ( <i>i</i> = C number in alkyl chain)
Bi	Biphenyl
F	Fluorene
C <sub>i</sub> -PH	Alkyl phenol ( <i>i</i> = C number in alkyl chain)
P	Phenanthrene
A	Anthracene
C <sub>i</sub> -P	Alkyl phenanthrene ( <i>i</i> = C number in the alkyl-chain)
UCM	Unresolved complex mixture

<sup>a</sup> Methyl ester.

<sup>b</sup> Dimethyl ester.

after the TMAH treatment. Benzene and alkyl benzenes, naphthalene and methyl naphthalenes remained prominent upon pyrolysis with and without TMAH. The relative abundances of selected aromatic and aliphatic compounds for the untreated leaf of

*N. penalveri* are summarized in Fig. 5a. The aromatic compounds selected are benzene, alkyl benzenes, naphthalene, alkyl naphthalenes. Selected aliphatic compounds are *n*-alkanes/*n*-alkenes in the case of Py-GC-MS; they additionally include FAMES and  $\alpha$ - $\omega$ -alkanedioic acid MEs in the case of THM-GC-MS.

The relative abundances of selected aromatic and aliphatic compounds upon Py-GC-MS and THM-GC-MS yield similar features for untreated leaf of *N. penalveri* and *F. turolensis* from the same rock layer (Rubielos; Fig. 5a and b). In the case of *F. turolensis* material, we additionally investigated the effect of the treatment used to extract the cuticle from the rock matrix and bleach it. Upon Py-GC-MS, both untreated leaves and bleached cuticles yield prominent aromatic compounds (mainly alkyl benzenes, naphthalenes, phenol, alkyl phenols) and *n*-alkanes/*n*-alkenes (Fig. 5a). The distribution of *n*-alkanes/*n*-alkenes (not shown) is quite similar to those for untreated leaves of *N. penalveri*. Upon THM-GC-MS, the pyrograms from bleached and untreated material both show a predominance of aliphatic compounds (Figs. 5a, 6 and 7). The *n*-alkanes/*n*-alkenes from the untreated leaf have the highest abundance for the shortest chain compounds (at C<sub>9</sub>–C<sub>12</sub>) and at C<sub>29</sub> (Fig. 6b). They largely decrease after bleaching and then show only very weak peaks (Fig. 7b). The untreated and the bleached material afforded prominent series of alkanedioic and alkenoic FAMES ranging from C<sub>5</sub> to C<sub>32</sub>, with distributions very similar to those observed for untreated leaf from *N. penalveri* (Figs. 3 and 4). The relative proportion of  $\alpha$ - $\omega$ -alkanedioic acid MEs (Fig. 5a) has very low values for untreated leaf and largely increases for bleached material. The *m/z* 74 chromatogram (Figs. 6c and 7c) points towards a slight relative increase in shorter chain (C<sub>6</sub>–C<sub>7</sub>) FAMES after bleaching. The untreated material shows trace amounts of alkan-2-ones ranging from C<sub>7</sub> to C<sub>11</sub>, while the bleached material afforded very weak peaks from short chain methoxyalkanoic acids. Alkyl benzenes are present in the untreated leaf pyrogram and largely decrease after bleaching. As a whole, the THM-GC-MS pyrograms from the bleached cuticle show a simplified distribution dominated overall by aliphatic compounds.

THM-GC-MS was also performed on untreated or bleached materials of *Frenelopsis alata* from the other level (Uña-3). The relative abundances of aromatic and aliphatic compounds from THM-GC-MS are shown in Fig. 5. As documented in Fig. 5 and by *m/z* 74 and 57 chromatograms (Appendix A), *F. alata* material from Uña-3 shows features quite similar to those observed for *F. turolensis* from Rubielos.

Both leaves and bleached cuticles of *F. turolensis* from Rubielos were subject to solvent extraction so that kerogen could be analyzed. Solvent extract accounts for 2.5% (by wt) of initial material in the case of leaf and for 18% in the case of bleached cuticle. The leaf after solvent extraction shows fairly minor changes in relative abundance of selected aliphatic and aromatic compounds upon THM-GC-MS (Fig. 5b). Regarding the distribution of FAMES, the *m/z* 74 chromatogram (Fig. 8c) indicates loss of long chain FAMES (which occurred in minor amount before solvent extraction) with even/odd predominance and relative increase in C<sub>14</sub>–C<sub>16</sub> FAMES. Extraction of long chain FAs with even/odd predominance (C<sub>28</sub>–C<sub>32</sub>) is confirmed by GC-MS analysis of the solvent extract (Fig. 10a). There is also a relative loss of C<sub>27</sub>–C<sub>33</sub> *n*-alkanes/*n*-alkenes with odd/even predominance after solvent extraction, as shown by *m/z* 57 chromatograms (Figs. 6b and 9a).

The bleached cuticle after solvent extraction shows a large loss of  $\alpha$ - $\omega$ -alkanedioic acid MEs, a loss of FAMES and a relative increase in *n*-alkanes/*n*-alkenes and in aromatic compounds (Fig. 5c). The *m/z* 74 chromatogram after solvent extraction indicates fast and complete removal of  $\alpha$ - $\omega$ -alkanedioic acid MEs and of long chain FAMES with even predominance (C<sub>26</sub>–C<sub>30</sub>;

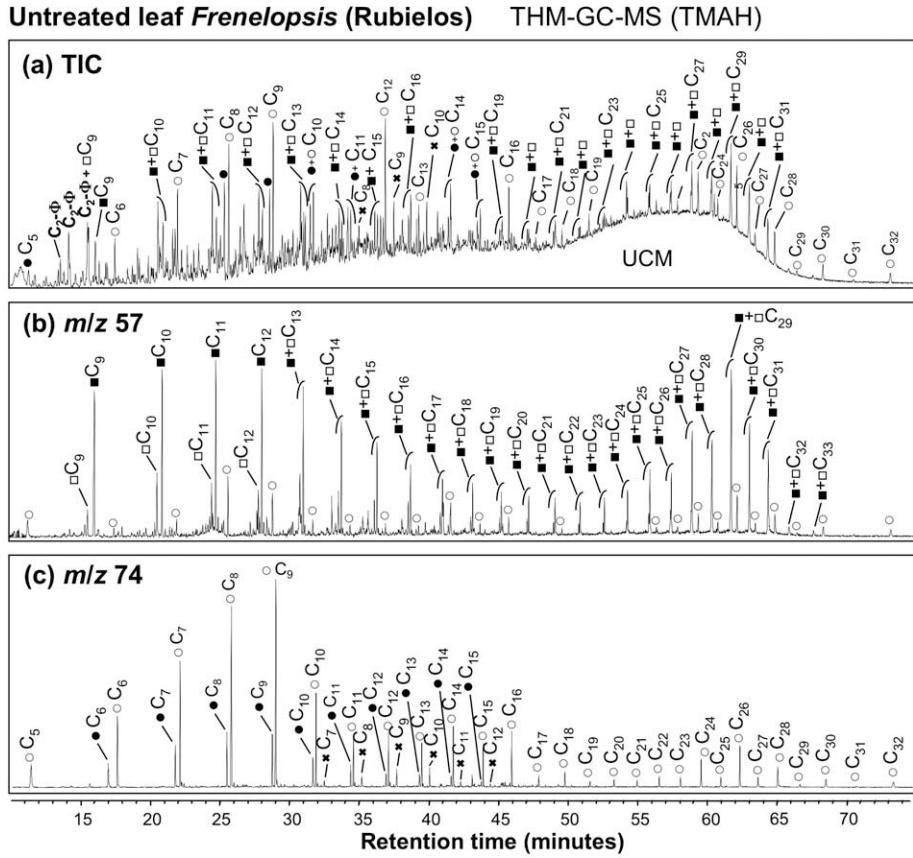


**Fig. 6.** Pyrograms of leaf of *Frenelopsis turoletensis* from Rubielos with TMAH: (a) TIC chromatogram, (b)  $m/z$  57 and (c)  $m/z$  74 chromatograms for untreated leaf. The  $m/z$  57 (e) and  $m/z$  74 (f) chromatograms are for DCM-extracted leaf.

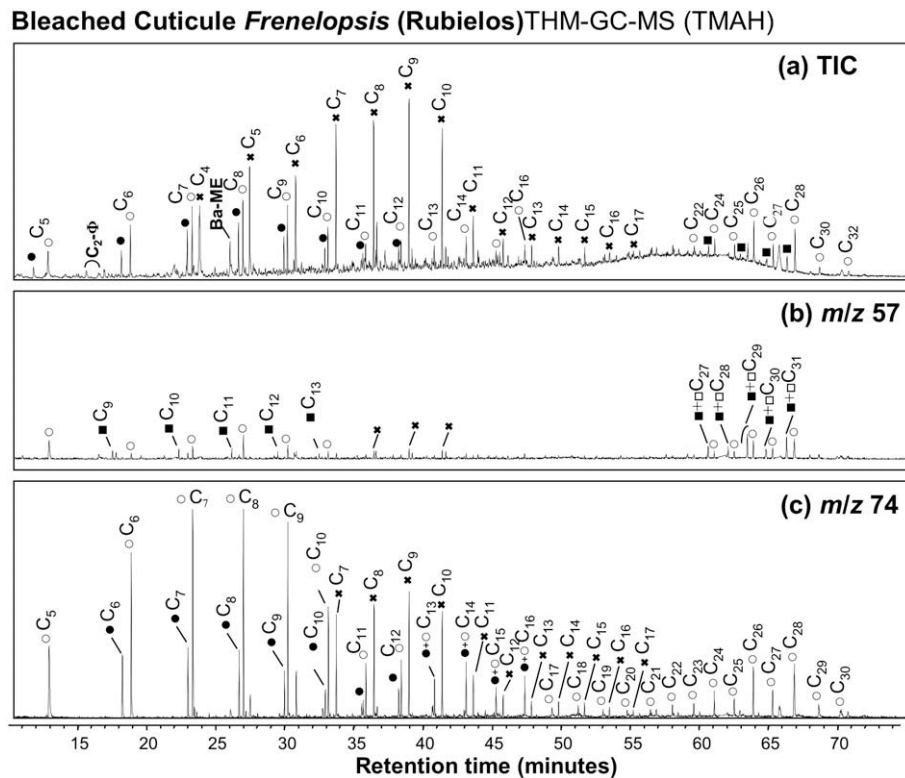


**Fig. 7.** Pyrograms of bleached cuticle of *Frenelopsis turoletensis* from Rubielos with TMAH: (a) TIC chromatogram, (b)  $m/z$  57 and (c)  $m/z$  74 chromatograms.

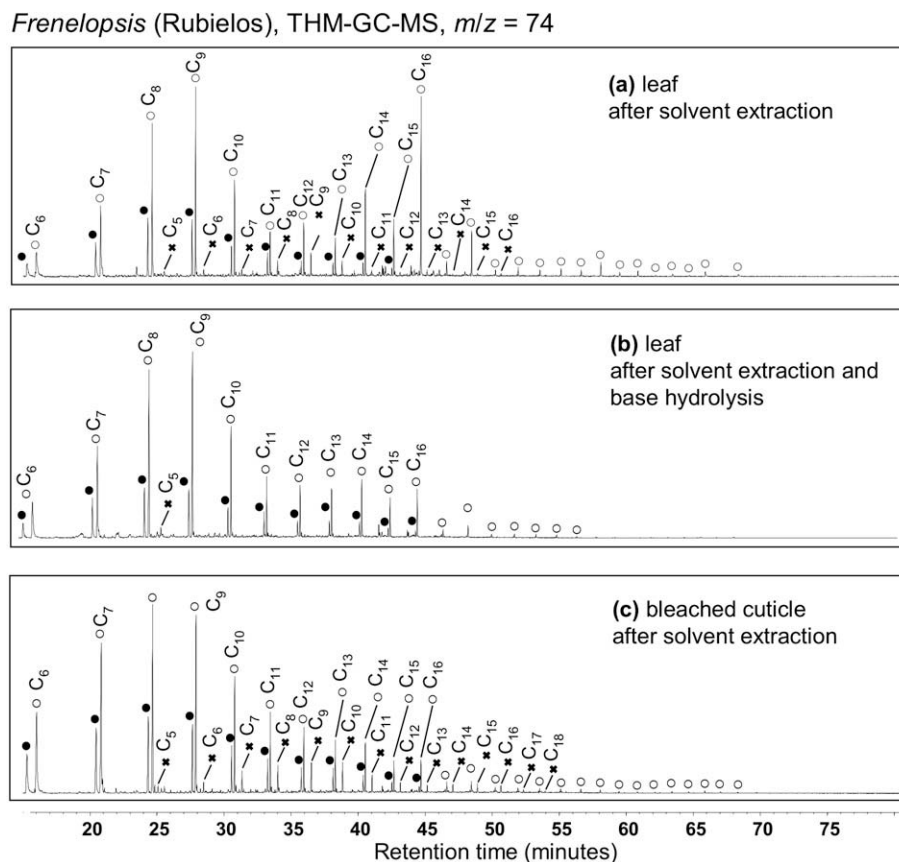


**Fig. 8.**  $m/z$  74 chromatograms upon THM-GC-MS for *Frenelopsis turolensis* from Rubielos (a) for leaf after solvent extraction, (b) for leaf after solvent extraction and base hydrolysis and (c) for bleached cuticle after solvent extraction.

Fig. 8c). This is consistent with the GC-MS analysis of the solvent extract (Fig. 10b).

Kerogen from leaf and bleached cuticle was subjected to base hydrolysis in order to investigate non-hydrolysable macromolecular components. The final residue after base hydrolysis represents 55% of kerogen in the case of the leaf and 90% in the case of the bleached cuticle. The leaf residue shows a decrease in FAMES relative to  $n$ -alkanes/ $n$ -alkenes (Fig. 5b). The distribution of aliphatic compounds was found to be similar in residues before and after base hydrolysis, except for the relative loss of  $C_{14}$ – $C_{16}$  FAMES (Figs. 8 and 9). For the bleached cuticle, the  $m/z$  74 (as well as the  $m/z$  57) chromatogram was found to be similar for kerogen (Figs. 8c and 10c) and for the final non-hydrolysable residue (Appendix B).

#### 4. Discussion

The main result of THM-GC-MS vs. conventional Py-GC-MS is that the former results in the series of alkanolic and alkenolic acids as well as  $\alpha$ - $\omega$ -alkanedioic acids for the untreated material. These compounds were not detected in previous studies based solely on conventional Py-GC-MS of similar material (Mösle et al., 1998). Unbleached cuticles of *Nehvizdya* (this study) and of Cretaceous Ginkgoales and *Frenelopsis* (Mösle et al., 1998) afforded quite similar product distributions upon conventional Py-GC-MS, that were devoid of FAs and diacids. Our results confirm previous findings from pyrolysis of *Frenelopsis* shoots with and without TMAH (Almendros et al., 1998). A noteworthy effect of the TMAH treatment has been found to be the release of additional series of FAMES. As acknowledged in previous studies (e.g. Hatcher and

Clifford, 1994; McKinney et al., 1996), the emergence of acids and diacids and the large decrease in  $n$ -alkanes and  $n$ -alkenes upon pyrolysis with TMAH is probably a result of several factors: (i) decarboxylation of FAs resulting in  $n$ -alkanes/ $n$ -alkenes doublets upon Py-GC-MS, (ii) loss of FAs on the apolar GC columns generally used for chromatographic separation of cuticular material and (iii) possible formation of alkyl benzenes from diunsaturated FAs upon Py-GC-MS, generated during flash pyrolysis (Saiz-Jimenez and Skelton, 1994; Hartgers et al., 1995; Faure et al., 2006). Combination of Py-GC-MS and infrared spectroscopy studies of *Frenelopsis* material (Mösle et al., 1998) has yielded pyrograms dominated by aromatic compounds and series of  $n$ -alkanes/ $n$ -alkenes, while the infrared spectra indicate the occurrence of oxygenated groups, presumably ketonic, and ionized or unionized carboxylate. The emergence of FAs upon pyrolysis with TMAH suggests that this discrepancy might be explained by recombination, decarboxylation or loss of FAs upon Py-GC-MS.

The pyrograms for untreated leaves show both aliphatic and aromatic compounds. Aromatic compounds partly originate from non-cuticular components rather than from the cuticle. High abundances of naphthalene and methyl naphthalenes, benzaldehyde and methyl benzaldehydes correspond to good morphological preservation of veins and resin bodies in leaves of *Nehvizdya*. Alkyl benzenes that have been reported as degradation products of lignin and lignocellulose (Hatcher et al., 1988, 1989) show a relative decrease on THM-GC-MS pyrograms of *Frenelopsis* material after bleaching and associated removal on non-cuticular organic residues.

Remarkably, the relative concentration and distribution of the aliphatic components released upon THM-GC-MS were found to

*Frenelopsis* (Rubielos), THM-GC-MS (TMAH),  $m/z = 57$

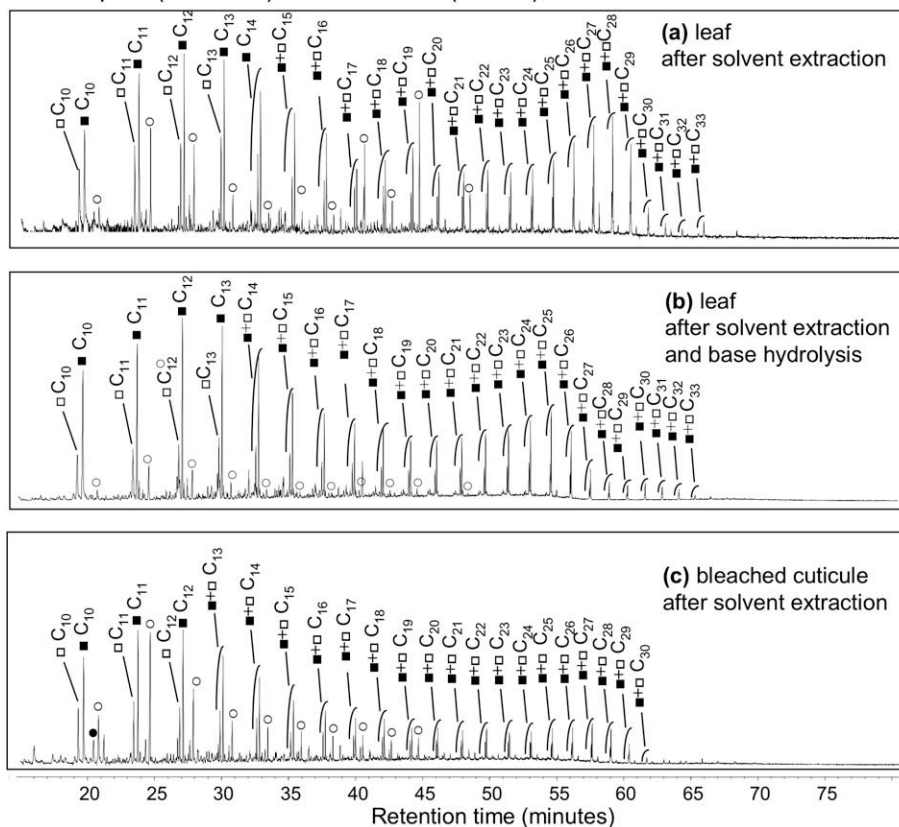


**Fig. 9.**  $m/z$  57 ion chromatograms upon THM-GC-MS for *Frenelopsis turolensis* from Rubielos (a) for leaf after solvent extraction, (b) for leaf after solvent extraction and base hydrolysis and (c) for bleached cuticle after solvent extraction.

○ Alkanolic acids      \*  $\alpha$ - $\omega$ -alkanedioic acids      ■  $n$ -alkanes

*Frenelopsis* (Rubielos), solvent extract, TIC, silylation-GC-MS

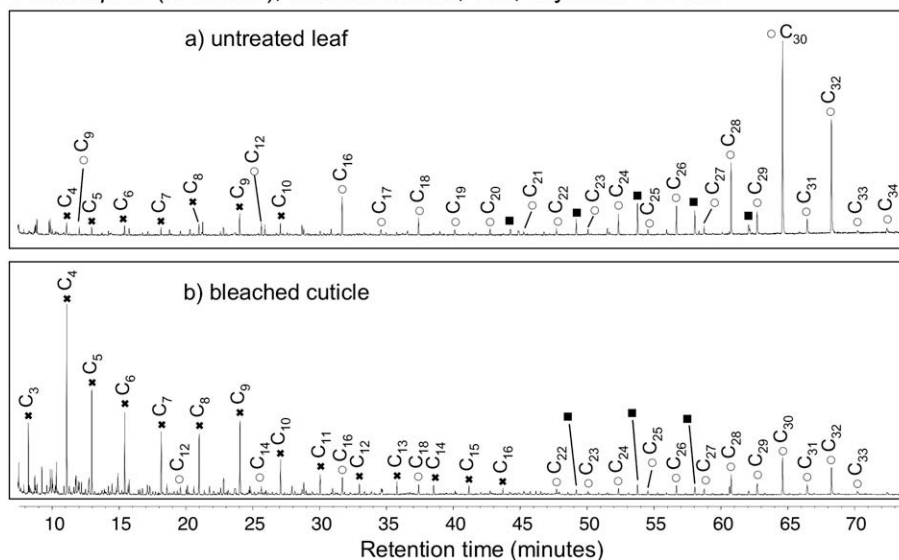


**Fig. 10.** Chromatograms of silylated extracts for (a) untreated leaf and (b) bleached cuticle.

be similar for *Frenelopsis* leaves from the two environments of deposition. They were also found to be very similar for two genera (*Frenelopsis*, *Nehvizdya*) preserved in the same depositional envi-

ronments. This suggests that the preservation state of aliphatic constituents of fossil leaves does not differ between the genera and the deposition environments studied.

Compared to untreated leaf, the bleached cuticle shows a marked relative increase in  $\alpha$ - $\omega$ -alkanedioic acid MEs upon THM-GC-MS. It also shows slight changes in the distribution of the FAMES. These changes can be attributed to (i) preferential loss of compounds other than diacids, i.e. aromatic compounds, FAs, *n*-alkanes/*n*-alkenes, and/or (ii) oxidation of hydrocarbon and FA components to diacids with the chemical treatment used to extract the cuticle from the mineral matrix and to bleach it. The relative decrease in aromatics, for instance, is consistent with the reported removal of aromatic moieties with  $\text{KClO}_3$ - $\text{HNO}_3$  treatment (Hemsley et al., 1996). Diacids appear as soluble, solvent extractable components that are essentially lost from the THM-GC-MS chromatograms after solvent extraction and that are found in the solvent extract. The detection of  $\alpha$ - $\omega$ -alkanedioic acid MEs from  $\text{C}_7$  to  $\text{C}_{11}$  in untreated material indicates that diacids occur in the fossilized leaf and are not solely produced by bleaching.

The THM-GC-MS data for untreated leaf, bleached cuticle and their kerogen fraction confirm the aliphatic nature of the fossil cuticle geopolymer and stress the importance of the FAs. The MEs of shorter chain FAs in the range  $\text{C}_6$ - $\text{C}_{16}$  appear as prominent components from the macromolecular material. They dominate the aliphatic assemblages of unbleached and bleached material, before and after solvent extraction. Long chain FAs with marked even/odd predominance and long chain *n*-alkanes/*n*-alkenes with odd/even predominance are present in small amounts in the pyrograms of the fossil leaf and cuticle, thereby suggesting the preservation of wax components. These components occur mainly as soluble, solvent extractable components; they are lost from THM-GC-MS pyrograms after solvent extraction and are found in GC-MS chromatograms of solvent extracts.

The THM-GC-MS data for residues after base hydrolysis of kerogen still indicate the occurrence of FAMES with distribution similar to that found for the kerogen fraction. They show a decrease in FAMES vs. *n*-alkanes/*n*-alkenes upon THM-GC-MS. This feature holds for unbleached as well as for bleached material. It suggests that part of the FAs was removed with base hydrolysis and that it might correspond to FAs bonded to the macromolecule by ester bonds. However, a lack of methoxylated aliphatic compounds upon THM-GC-MS points toward a scarcity of OH-substituted alkyl chains and ester bonds in the kerogen. Base hydrolysis is commonly used on modern plants to remove monomers from cutin polyesters but its effect on kerogen from fossil leaves had scarcely been documented (Gupta et al., 2007a-c). Gupta et al. (2007a-c) found no release of aliphatic FAs but noticed that partial alteration of the geopolymer could occur with base hydrolysis. In the case of our material, THM-GC-MS data before and after base hydrolysis rather suggest that partial alteration of the macromolecule with base hydrolysis could lead to removal of FA moieties that are not necessarily bonded via ester bonds and/or could favour the release of *n*-alkanes/*n*-alkenes upon THM-GC-MS.

The occurrence and distribution of pyrolysis products upon THM-GC-MS show major differences between the fossil cuticles and cuticular components from living plants. Cutan is a chemically resistant biopolymer left after wax, cutin and polysaccharide extraction from the cuticle of some living plants (Nip et al., 1986). Its selective preservation is thought to be one possible way of preservation for plant cuticle in the fossil record (Nip et al., 1986; Tegelaar et al., 1991; Boom et al., 2005; de Leeuw et al., 2006). Under THM conditions, it affords saturated FAMES in the range  $\text{C}_{15}$ - $\text{C}_{31}$ , with higher concentrations of the longer chain compounds, and a large number of trimethoxybenzenes (McKinney et al., 1996). The very low abundances of long chain alkanedioic acid MEs and the lack of trimethoxybenzene structures upon THM-GC-MS is evidence for cutan not being a significant component of *Frenelopsis* and *Nehvizdya* cuticles.

The absence of a clear cutan signature upon THM-GC-MS favours in this case the alternative/additional model of preservation via in situ polymerization of aliphatic moieties derived from the less resistant cuticular components cutin and wax (Tegelaar et al., 1991; Möslle et al., 1998; de Leeuw et al., 2006; Gupta et al., 2007a,b). Cutin from living plants yields essentially mono-hydroxy, monomethoxy, hexadecanoic acid and dimethoxy hexadecanoic acid MEs upon THM-GC-MS (de Leeuw and Baas, 1993; del Rio and Hatcher, 1998). These compounds are derived from dihydroxy hexadecanoic acids of the cutin polyester. In modern conifers for instance, cutin has a dominance of 9-16- or 10,16-dihydroxyhexadecanoic acids and lesser amounts of other hydroxylated FAs ranging from  $\text{C}_{14}$  to  $\text{C}_{18}$  (Hunneman and Eglinton, 1972; Goñi and Hedges, 1990). In the fossil leaves and cuticles studied here, the FAME data show an apparent cutin signal, with a relative maximum at  $\text{C}_{16}$ . One important difference between the fossil cuticles and cutin is, however, a lack of alcohol methyl ethers and methoxylated FAs. A lack of these compounds in the fossil cuticles points toward a scarcity of OH-substituted alkyl chains and ester bonds. Another important difference concerns the distribution of the FAMES. The highest abundances of  $\text{C}_8$ - $\text{C}_9$  FAMES in the fossil cuticles suggests that bridging between the FA units might preferentially occur at the C-8/C-10 position of the units.

The lack of OH-substituted alkyl chains upon THM-GC-MS supports the hypothesis of newly formed, non-ester, cross linkages between FA units in the fossil cuticles (Tegelaar et al., 1991; Möslle et al., 1998; Almendros et al., 1999; de Leeuw et al., 2006; Gupta et al., 2007a-c). The occurrence of short chain FAMES and dicarboxylic acid MEs upon THM has been used as evidence for preservation via oxidative lipid polymerization in the case of dinocasts (Versteegh et al., 2004; de Leeuw, 2007), i.e. internal contents of fossil dinoflagellates with exceptional morphological preservation. Oxidative lipid polymerization involves the autooxidation of unsaturated  $\text{C}_{18}$  FA components of triacylglycerols, resulting in extensive cross linking, together with oxidative degradation and formation of short chain mono and dicarboxylic acids. The pyrograms from *Frenelopsis* and *Nehvizdya* leaves and from dinocasts (Versteegh et al., 2004) share common features. The THM-GC-MS pyrograms yield quite similar distributions of short chain mono acids (dominantly  $<\text{C}_{16}$ ), diacids (peaking at  $\text{C}_7$ - $\text{C}_{11}$ ). The Py-GC-MS pyrograms for both materials show alkan-2-ones and dominant series of *n*-alkanes/*n*-alkenes series with relative maxima at  $\text{C}_8$ - $\text{C}_{10}$ . The pathway of lipid preservation via oxygen incorporation is a likely mechanism for the preservation of cell contents and membranes (Versteegh et al., 2004; de Leeuw et al., 2006). It is more widely viewed as an important process in kerogen formation under relatively oxic conditions, with unsaturated sites being directly derived from biological lipid precursors or originating from diagenetic processes (Riboulleau et al., 2001). It has been shown by Gupta et al. (2007b) that lipids from leaf cell tissues contribute to the formation of the aliphatic geopolymer in the fossil leaf. This contribution might partly explain the similarity between the THM-GC-MS data from dinocasts and fossil leaves. In situ polymerization is invoked as a diagenetic pathway to explain the formation of the aliphatic polymer found in fossil cuticles (Tegelaar et al., 1991; de Leeuw et al., 2006; Gupta et al., 2007a-c; de Leeuw, 2007) and is a likely preservation pathway involved in the fossil cuticles studied here.

## 5. Conclusions

THM-GC-MS data confirm the aliphatic nature of the fossil cuticle geopolymer and stress the importance of the fatty acids. In the case of the Cretaceous Ginkgoales and Coniferales studied, evidence from THM-GC-MS of leaf macromolecular material

supports the preservation model via in situ polymerization rather than via selective preservation of cutan. The fatty acid distribution remarkably maximizes at C<sub>8</sub>–C<sub>9</sub>, suggesting preferential fragmentation from the macromolecular network at this position during pyrolysis. This would be in accord with unsaturated fatty acids having undergone some kind of cross linking at C<sub>9</sub>–C<sub>10</sub>. At this stage of the study, there are no definite arguments to establish the exact nature of the cross bonds between aliphatic moieties.

The material studied shows excellent morphological preservation of the cuticle, either unbleached or bleached. In contrast, the THM-GC–MS data confirm that important changes in chemical composition occur between modern and fossil cuticle. The data also document that significant changes occur after bleaching, i.e. increase in short chain diacids, and decrease in aromatic moieties and *n*-alkanes/*n*-alkenes. These changes appear to be due to the loss of extracuticular material, mainly aromatic moieties, and to the oxidation of extracuticular–cuticular components.

The observations have implications for the interpretation of carbon isotope signals in fossil plants. In the case of selective preservation of cutan, the carbon isotope signature of fossil cuticle should be directly inherited from that of the plant cutan. In the case of in situ preservation, palaeoenvironmental interpretation of isotope variations should be better made for fossil cuticles showing a similar state of preservation. Data from THM-GC–MS can help control the state of preservation. The pyrolysis data also point towards a large variation in the ratio between aliphatic and aromatic moieties that depends on the leaves studied and on the kind of pre-treatment; this might be a source of isotopic variation.

## Acknowledgements

This project was funded through research grants awarded to A.M.A., B.G., R.M. and F.T. from the CNRS-INSU (ECLIPSE programme) and from the Institut Français de la Biodiversité (IFB) (2003–11). B.G. was supported by the Spanish Ministerio de Educación y Ciencia (CGL2005-00046 and CGL2005-01121), the Catalan government (2005SGR-00890) and the French Agence Nationale de la Recherche (project AMBRACE, BLAN07-1-184190). Suggestions and comments from N.S. Gupta, J.W. de Leeuw, P. van Bergen, S. Derenne and an anonymous reviewer greatly contributed to improving the manuscript.

## Appendix A. Supplementary material

Supplementary data associated with this article can be found, in the online version, at doi:10.1016/j.orggeochem.2009.04.006.

Associate Editor—K.J.G. Nierop

## References

- Almendros, G., González-Vila, Martín, F., Sanz, J., Álvarez-Ramis, C., 1998. Appraisal of pyrolytic technique on different forms of organic matter from a Cretaceous basement in Central Spain. *Organic Geochemistry* 28, 613–623.
- Almendros, G., Dorado, J., Sanz, J., Álvarez-Ramis, C., Fernández-Marrón, M.T., Archangelsky, S., 1999. Compounds released by sequential chemolysis from cuticular remains of the Cretaceous gymnosperm *Squamastrobos tigrens* (Patagonia, the Argentine). *Organic Geochemistry* 30, 623–634.
- Boom, A., Sinnighe Damsté, J.S., de Leeuw, J.W., 2005. Cutan, a common aliphatic biopolymer in cuticles of drought-adapted plants. *Organic Geochemistry* 36, 595–601.
- Briggs, D.E.G., 1999. Molecular taphonomy of animal and plant cuticles: selective preservation and diagenesis. *Philosophical Transactions of the Royal Society of London. Series B: Biological Sciences* 354, 7–16.
- Challinor, J.M., 1989. A pyrolysis-derivatization – gas chromatography technique for the elucidation of some synthetic polymers. *Journal of Analytical and Applied Pyrolysis* 16, 323–333.
- Challinor, J.M., 1991. Structure determination of alkyd resins by simultaneous pyrolysis methylation. *Journal of Analytical and Applied Pyrolysis* 18, 233–244.
- Challinor, J.M., 1994. On the mechanism of high temperature reactions of quaternary ammonium hydroxides with polymers. *Journal of Analytical and Applied Pyrolysis* 29, 223–224.
- Daviero, V., Gomez, B., Philippe, M., 2001. Uncommon branching pattern within conifers: *Frenelopsis turoloensis*, a Spanish Early Cretaceous Cheirolepidiaceae. *Canadian Journal of Botany* 79, 1400–1408.
- de Leeuw, J.W., Baas, M., 1993. The behavior of esters in the presence of tetramethylammonium salts at elevated temperatures; flash pyrolysis or flash chemolysis? *Journal of Analytical and Applied Pyrolysis* 26, 175–184.
- de Leeuw, J.W., Versteegh, G.J.M., van Bergen, P.F., 2006. Biomacromolecules of algae and plants and their fossil analogues. *Plant Ecology* 182, 209–233.
- de Leeuw, J.W., 2007. On the origin of sedimentary aliphatic macromolecules: a comment on recent publications by Gupta et al.. *Organic Geochemistry* 38, 1585–1587.
- del Rio, J.C., Hatcher, P.G., 1998. Analysis of aliphatic biopolymers using thermochemolysis with tetramethylammonium hydroxide (TMAH) and gas chromatography–mass spectrometry. *Organic Geochemistry* 29, 1441–1451.
- Faure, P., Schlepp, L., Mansuy-Huault, L., Elie, M., Jardé, E., Pelletier, M., 2006. Aromatization of organic matter induced by the presence of clays during flash pyrolysis-gas chromatography–mass spectrometry (Py-GC–MS). *Journal of Analytical and Applied Pyrolysis* 75, 1–10.
- Finch, P., Freeman, G., 2001. Simulated diagenesis of plant cuticles – implications for organic fossilisation. *Journal of Analytical and Applied Pyrolysis* 58–59, 229–235.
- Gomez, B., Martín-Closas, C., Barale, G., Thévenard, F., 2000. A new species of *Nehvizdya* (Ginkgoales) from the Lower Cretaceous of the Iberian Range. *Review of Palaeobotany and Palynology* 111, 49–70.
- Gomez, B., Martín-Closas, C., Méon, H., Thévenard, F., Barale, G., 2001. Plant taphonomy and palaeoecology in the lacustrine Uña delta (Late Barremian, Iberian Ranges, Spain). *Palaeogeography, Palaeoclimatology, Palaeoecology* 170, 133–148.
- Gomez, B., Martín-Closas, C., Barale, G., de Porta, N.S., Thévenard, F., Guignard, G., 2002. *Frenelopsis* (Coniferales, Cheirolepidiaceae) and related male organ genera from the lower Cretaceous of Spain. *Palaeontology* 43, 997–1036.
- Goñi, M.A., Hedges, J.I., 1990. Potential applications of cutin-derived CuO reaction products for discriminating vascular plant sources in natural environments. *Geochimica et Cosmochimica Acta* 54, 3073–3081.
- Gupta, N.S., Collinson, M.E., Briggs, D.E.G., Evershed, R.P., Jack, K.S., Pancost, R.D., 2006. Reinvestigation of the occurrence of cutan in plants: implications for the fossil leaf record. *Paleobiology* 32, 432–449.
- Gupta, N.S., Briggs, D.E.G., Collinson, M.E., Evershed, R.P., Michels, R., Jack, K.S., Pancost, R.D., 2007a. Experimental evidence for the formation of geomacromolecules from plant leaf lipids. *Organic Geochemistry* 38, 28–36.
- Gupta, N.S., Briggs, D.E.G., Collinson, M.E., Evershed, R.P., Michels, R., Jack, K.S., Pancost, R.D., 2007b. Evidence for the *in-situ* polymerisation of labile organic compounds during the preservation of fossil leaves: implications for organic matter preservation. *Organic Geochemistry* 38, 499–522.
- Gupta, N.S., Briggs, D.E., Collinson, M.E., Evershed, R.P., Michels, R., Pancost, R.D., 2007c. Reply to De Leeuw Comment on the origin of sedimentary aliphatic macromolecules. *Organic Geochemistry* 38, 1588–1591.
- Gupta, N.S., Cambra-Moo, O., Briggs, D.E., Love, G.D., Fregenal-Martínez, M.A., Summons, R.E., 2008. Molecular taphonomy of microfossils from the Cretaceous Las Hoyas Formation, Spain. *Cretaceous Research* 29, 1–8.
- Hatcher, P.G., Lerch III, H.E., Kotra, R.K., Verheyen, T.V., 1988. Pyrolysis-GC–MS of a series of degraded woods and coalified logs that increase in rank from peat to subbituminous coal. *Fuel* 67, 1069–1075.
- Hatcher, P.G., Lerch III, H.E., Verheyen, T.V., 1989. Organic geochemical studies of the transformation of gymnosperm xylem during peatification and coalification to subbituminous coal. *International Journal of Coal Geology* 13, 65–97.
- Hatcher, P.G., Clifford, D.J., 1994. Flash pyrolysis and *in situ* methylation of humic acids from soils. *Organic Geochemistry* 21, 1081–1092.
- Hartgers, W.A., Sinnighe Damsté, J.W., de Leeuw, J.W., 1992. Identification of C<sub>2</sub>–C<sub>4</sub> alkylated benzenes in flash-pyrolysates of kerogens, coals and asphaltenes. *Journal of Chromatography A* 606, 211–220.
- Hartgers, W.A., Sinnighe Damsté, J.S., de Leeuw, J.W., 1995. Curie-point pyrolysis of sodium salts of functionalized fatty acids. *Journal of Analytical and Applied Pyrolysis* 34, 191–217.
- Hemsley, A.R., Scott, A.C., Barrie, P.J., Chaloner, W.G., 1996. Studies of fossil and modern spore wall biomacromolecule using <sup>13</sup>C solid state NMR. *Annals of Botany* 78, 83–94.
- Hunneman, D.H., Eglinton, G., 1972. The constituent acids of gymnosperm cutins. *Phytochemistry* 11, 1989–2001.
- Ishiwatari, M., Ishiwatari, R., Sakashita, H., Tatsumi, T., 1995. Application of pyrolysis-gas chromatography to the study of chlorophyll-*a*. Effect of clay minerals. *Journal of Analytical and Applied Pyrolysis* 32, 153–160.
- Kerp, H., 1990. The study of fossil gymnosperms by means of cuticle analysis. *Palaios* 5, 548–569.
- Kögel-Knabner, I., de Leeuw, J.W., Tegelaar, E.W., Hatcher, P.G., Kerp, H., 1994. A lignin-like polymer in the cuticle of spruce needles: implications for the humification of spruce litter. *Organic Geochemistry* 21, 1219–1228.
- Kokinos, J.P., Eglinton, T.I., Goni, M.A., Boon, J.J., Martoglyio, P.A., Anderson, D.M., 1998. Characterization of a highly resistant biomacromolecular material in the cell wall of a marine dinoflagellate resting cyst. *Organic Geochemistry* 28, 265–288.
- McKinney, D.E., Bortiatinski, J.M., Carson, D.M., Clifford, D.J., de Leeuw, J.W., Hatcher, P.G., 1996. Tetramethylammonium hydroxide (TMAH) thermochemolysis of the

- aliphatic biopolymer cutan: insights into the chemical structure. *Organic Geochemistry* 24, 641–650.
- Mösle, B., Fich, P., Collinson, M., Scott, A.C., 1997. Comparison of modern and fossil plant cuticles by selective chemical extraction monitored by flash pyrolysis-gas chromatography-mass spectrometry and electron microscopy. *Journal of Analytical and Applied Pyrolysis* 40–41, 585–597.
- Mösle, B., Collinson, M.E., Finch, P., Stankiewicz, A., Scott, A.C., Wilson, R., 1998. Factors influencing the preservation of plant cuticles: a comparison of morphology and chemical composition of modern and fossil examples. *Organic Geochemistry* 29, 1369–1380.
- Nip, M., Tegelaar, E.W., Brinkhuis, H., de Leeuw, J.W., Schenck, P.A., Holloway, P.J., 1986. Analysis of modern and fossil plant cuticles by Curie point Py-GC and Curie point Py-GC-MS: recognition of a new, aliphatic and resistant biopolymer. *Organic Geochemistry* 10, 679–778.
- Riboulleau, A., Derenne, S., Largeau, C., Baudin, F., 2001. Origin of contrasting features and preservation pathways in kerogens from Kashpir oil shales (Upper Jurassic, Russian platform). *Organic Geochemistry* 32, 647–665.
- Skelton, P.W., 2003. *The Cretaceous World*. Cambridge University Press, pp. 360.
- Saiz-Jimenez, C., Skelton, B.W., 1994. Analytical pyrolysis of humic substances. Pitfalls, limitations and possible solutions. *Environmental Science and Technology* 28, 1773–1780.
- Stankiewicz, B.A., Briggs, D.E.G., Michels, R., Collinson, M., Flannery, M.B., Evershed, R.P., 2000. Alternative origin of aliphatic polymer in kerogen. *Geology* 28, 559–562.
- Tegelaar, E.W., Kerp, H., Vissler, H., Schenck, P.A., de Leeuw, J.W., 1991. Bias of the paleobotanical record as a consequence of variations in the chemical compositions of higher plant cuticles. *Paleobiology* 17, 133–144.
- Versteegh, G.J.M., Blokker, P., Wood, G.D., Collinson, M.E., Sinninghe Damsté, J.S., de Leeuw, J.W., 2004. An example of oxidative polymerisation of unsaturated fatty acids as a preservation pathway for dinoflagellate organic matter. *Organic Geochemistry* 35, 1129–1139.
- Watson, J., 1977. Some Lower Cretaceous conifers of the Cheirolepidiaceae from the USA and England. *Palaeontology* 20, 715–749.
- Wenclawiak, B.W., Jensen, T.E., Richert, J.F.O., 1993. GC/MS-FID analysis of BSTFA derivatized polar components of diesel particulate matter (NBS SRM-1650) extract. *Fresenius Journal of Analytical Chemistry* 346, 808–812.